

Stable Inversion of Discrete-Time Nonlinear Maximum-Phase Systems*

SONG LI and DAVID G. TAYLOR

Georgia Institute of Technology
School of Electrical and Computer Engineering
Atlanta, GA 30332-0250 USA

Abstract: This paper formulates and solves the problem of stable inversion for a class of discrete-time nonlinear systems possessing either completely stable or completely unstable zero dynamics. Given a desired output trajectory, the new stable inversion method determines bounded desired trajectories for the input and state variables that satisfy the plant state and output equations. The desired input and state trajectories may be used as feedforward signals for tracking control purposes, and/or they may be used to study the influence of plant parameters on control requirements. The stable inversion process involves numerical calculations with Newton iterations and is causal for minimum-phase systems and noncausal for maximum-phase systems. An application to an electronic power conversion circuit illustrates the significant benefits of computing the feedforward input using stable inversion instead of the more traditional dc-gain method, including large reductions in peak transient error, settling time and overshoot.

Keywords: digital control, feedforward control, nonlinear systems, nonminimum-phase systems, power converters.

1 Introduction

Asymptotic output tracking is a challenging problem when dealing with nonlinear nonminimum-phase systems. Consider the continuous-time case. Input-output linearization [3] provides the desired asymptotic tracking property but fails to provide bounded internal plant states and bounded plant input. Nonlinear output regulation [4] provides both internal stability and asymptotic tracking for trajectories generated by an exosystem, but requires solution of a set of nonlinear partial differential equations for implementation. The stable inversion method [1, 2] provides perfect tracking without transient error through the combination of a bounded (but non-causal) feedforward control and a feedback control to stabilize the desired trajectory.

In this paper, the stable inversion method is extended to discrete-time nonlinear maximum-phase systems; the simpler minimum-phase case is included as well. Such an extension is believed to be useful for practical applications in which the non-

linear control system is to be implemented digitally. The concepts of relative degree, normal form and inverse dynamics for nonlinear discrete-time systems are first established. Since the system exhibits a nonlinear dependence on both the state and the input, the inverse dynamics cannot generally be expressed in explicit form. A characterization of inverse dynamics stability is provided, and a Newton iteration method is developed to obtain a bounded solution to the implicit inverse dynamics. Finally, the new discrete-time stable inversion method is applied to the nonlinear maximum-phase sampled-data model of a pulse-width modulated power conversion circuit to illustrate the possibility of exact tracking with boundedness of all signals through the use of non-causal stable inversion and pre-actuation.

2 Problem Statement

Throughout this paper, the focus is on single-input single-output nonlinear discrete-time systems of the form

$$x_{k+1} = F(x_k, u_k) \quad (1)$$

$$y_k = h(x_k) \quad (2)$$

*This work was supported in part by the National Science Foundation under grant ECS-9158037 and by the Office of Naval Research under grant N00014-96-1-0926.

where $x \in R^n$, $u \in R$, $y \in R$, and F and h are smooth, with equilibrium point (\bar{x}, \bar{u}) defined by $\bar{x} = F(\bar{x}, \bar{u})$, and with equilibrium output $\bar{y} = h(\bar{x})$. The model (1)–(2) may represent an inherently discrete-time process or it may define the discrete-time dynamics of a sampled-data system. Due to the introduction of so-called sampling zeros in sampled-data models, the possibility of system (1)–(2) being nonminimum-phase is very high.

The primary objective of this paper is to extend the concept of stable inversion to nonlinear discrete-time systems of the form (1)–(2). More precisely, given a bounded desired output trajectory y_k^d , the goal is to determine corresponding bounded desired trajectories for the input and state variables, i.e. to determine bounded u_k^d and x_k^d such that the constraints

$$x_{k+1}^d = F(x_k^d, u_k^d) \quad (3)$$

$$y_k^d = h(x_k^d) \quad (4)$$

are satisfied for all k . If such bounded desired trajectories for the input and state variables can be found, then a reasonable tracking control method would be to use a combination of feedforward (for tracking performance) and feedback (for stabilization), e.g.

$$u_k = u_k^d + K(x_k^d - x_k)$$

where the row vector K is determined using any suitable stabilization method.

3 Stable Inversion

3.1 Relative Degree

Considering system (1)–(2), note that y_k cannot be directly influenced by u_k since there is no direct throughput term in the output equation. On the other hand, since

$$y_{k+1} = h(F(x_k, u_k))$$

it is clear that y_{k+1} can possibly be influenced by u_k , depending on the nature of the nested function $h(F(x, u))$. In the event that y_{k+1} is not influenced by u_k , it is possible to write

$$y_{k+2} = h(F(F(x_k, u_k), \star))$$

where \star represents the fact that the value of $h(F(x, u))$ does not depend on the value of u , i.e. \star only serves as a place holder. The nature of the nested function $h(F(F(x, u), \star))$ would then determine whether or not y_{k+2} is influenced by u_k . Following this logic, one could in principle determine how much delay is present between the input and the output of system (1)–(2). Such information is intuitively important when attempting to determine the input required to excite a given output.

The discussion above motivates the need for a formal definition of relative degree. Associated with the system (1)–(2) is the family of iterated functions

$$\hat{F}^i(x, u) := \underbrace{F^\star \circ \cdots \circ F^\star}_{i-1} \circ F^u(x), \quad i \geq 1$$

where \circ denotes the usual composition of functions, $F^u(\cdot) := F(\cdot, u)$ and \star is used as a place holder. The system (1)–(2) is said to have *relative degree* $r > 0$ at (x_\star, u_\star) if for all (x, u) near (x_\star, u_\star)

$$\frac{\partial}{\partial u} \{h \circ \hat{F}^i(x, u)\} \equiv 0, \quad 0 < i < r$$

and

$$\frac{\partial}{\partial u} \{h \circ \hat{F}^r(x, u)\} \neq 0$$

Some systems do not possess a well-defined relative degree. For those that do, $k = r$ is the first instant of time at which the output is affected by the input applied at $k = 0$.

3.2 Normal Form

If the system (1)–(2) does in fact have relative degree r at (\bar{x}, \bar{u}) , then $r \leq n$ and it is possible to define locally a change of state coordinates as follows. Set r functions of x by

$$\begin{aligned} \phi_1(x) &:= h(x) \\ \phi_2(x) &:= h \circ \hat{F}^1(x, \star) \\ &\vdots \\ \phi_r(x) &:= h \circ \hat{F}^{r-1}(x, \star) \end{aligned}$$

noting that the relative degree assumption guarantees that these functions depend only on x and not on u . If $r < n$, choose $n - r$ additional smooth functions of x , say $\phi_{r+1}(x), \dots, \phi_n(x)$, such that the mapping

$$\varphi(x) := \begin{bmatrix} \phi_1(x) \\ \phi_2(x) \\ \vdots \\ \phi_n(x) \end{bmatrix}$$

where

$$\begin{aligned} \varphi_1(x) &:= [\phi_1(x) \quad \cdots \quad \phi_r(x)]' \\ \varphi_2(x) &:= [\phi_{r+1}(x) \quad \cdots \quad \phi_n(x)]' \end{aligned}$$

satisfies

$$\det \frac{\partial \varphi}{\partial x} \Big|_{\bar{x}} \neq 0$$

and where $\varphi(\bar{x}) = 0$. The change of state coordinates

$$\begin{bmatrix} \zeta \\ \eta \end{bmatrix} := \begin{bmatrix} \varphi_1(x) \\ \varphi_2(x) \end{bmatrix}$$

transforms (1)–(2) into

$$\zeta_{i,k+1} = \zeta_{i+1,k}, \quad i = 1, \dots, r-1 \quad (5)$$

$$\zeta_{r,k+1} = \alpha(\zeta_k, \eta_k, u_k) \quad (6)$$

$$\eta_{k+1} = \beta(\zeta_k, \eta_k, u_k) \quad (7)$$

$$y_k = \zeta_{1,k} \quad (8)$$

where

$$\begin{aligned}\alpha(\zeta, \eta, u) &:= h \circ \hat{F}^r(\varphi^{-1}(\zeta, \eta), u) \\ \beta(\zeta, \eta, u) &:= \varphi_2(F(\varphi^{-1}(\zeta, \eta), u))\end{aligned}$$

Because of the special significance of the ζ coordinates imposed through the selection of $\varphi_1(x)$, system (5)–(8) is referred to as the *normal form* of system (1)–(2). Although these two representations of the system are mathematically equivalent, the normal form is more useful for certain analyses, since the coordinates ζ and η can be associated with external and internal behaviors, respectively.

3.3 Inverse Dynamics

The inverse dynamics of system (1)–(2) is a related dynamic system, having desired output trajectory signals y_k^d, \dots, y_{k+r}^d as inputs and a corresponding input trajectory u_k as output. The stable inversion problem naturally requires the formulation of the inverse dynamics, and the normal form (5)–(8) is useful for this purpose. The constraint that the output exactly track the desired output

$$y_k \equiv y_k^d$$

implies from (8) and (5) the constraint

$$\zeta_k = \zeta_k^d := [y_k^d \ \cdots \ y_{k+r-1}^d]'$$

and from (6) and (7) the constraints

$$y_{k+r}^d = \alpha(\zeta_k^d, \eta_k, u_k) \quad (9)$$

$$\eta_{k+1} = \beta(\zeta_k^d, \eta_k, u_k) \quad (10)$$

The dynamic system (9)–(10) is referred to as the *inverse dynamics* of the original system (1)–(2). Note that (9) represents an implicit output equation whereas (10) represents an implicit state equation. The output equation (9) is implicit since the function α depends on u_k in a nonlinear way; hence, it is not generally possible to solve explicitly for the output u_k of the inverse dynamics. Similarly, the state equation (10) is implicit in the sense that the function β depends on u_k , and this dependence cannot be explicitly replaced by an equivalent dependence on the signals of interest ($y_{k+r}^d, \zeta_k^d, \eta_k$) because of the nonlinearity of α with respect to u_k .

The state coordinate change $\varphi(x)$ reveals a constraint on the initial state x_0 of the original system (1)–(2) required to meet the previously discussed output tracking property. Specifically, since the value of ζ_k is constrained by the desired output trajectory for all time including $k = 0$, it follows that x_0 must satisfy

$$x_0 = \varphi^{-1}(\zeta_0^d, \eta_0), \quad \eta_0 \text{ free}$$

Since the choice of η_0 is completely free, the inverse dynamics analysis indicates that there are an infinite number of ways to satisfy the output tracking

constraint $y_k \equiv y_k^d$, corresponding to the infinite number of possible choices for η_0 . Each possible choice for η_0 generates a distinct output-state trajectory $\{u_k, \eta_k\}$ for the inverse dynamics (9)–(10), and a corresponding distinct input-state trajectory $\{u_k, x_k\} = \{u_k, \varphi^{-1}(\zeta_k^d, \eta_k)\}$ for the original system (1)–(2).

3.4 Stability Characterization

The computational procedure for stable inversion recommended in this paper will be based on numerical solution of coupled nonlinear algebraic equations, and the determination of an appropriate initial condition η_0 will be handled automatically. To prepare for a discussion of this computational procedure, it is first necessary to assess the stability properties of the inverse dynamics, since these stability properties will influence the logic of the computational procedure. Assume that the desired output trajectory y_k^d belongs to a neighborhood of the equilibrium output \bar{y} and, for the sake of simplicity, assume further that $\bar{y} = 0$. In this case, the qualitative behavior of the inverse dynamics can be predicted most easily by analyzing the stability of a simpler autonomous dynamic system, namely the unforced inverse dynamics corresponding to $y_k^d = \bar{y} = 0$. Under this scenario, the inverse dynamics reduces to the autonomous form

$$0 = \alpha(0, \eta_k, u_k) \quad (11)$$

$$\eta_{k+1} = \beta(0, \eta_k, u_k) \quad (12)$$

The dynamic system (11)–(12) is referred to as the *zero dynamics* of the original system (1)–(2), since it represents (in the k -domain) the nonlinear analog of the notion of zeros for linear systems (in the z -domain). Note that, as before, the nonlinearity of α with respect to u_k prohibits any explicit representation for the zero dynamics.

Since $\varphi(\bar{x}) = 0$ by construction, the implicit zero dynamics (11)–(12) possesses an equilibrium at $\bar{\eta} = 0$. According to Lyapunov's indirect method, if $\bar{\eta} = 0$ is a hyperbolic equilibrium of (11)–(12), then the stability of this equilibrium may be determined through an investigation of the linear approximation of (11)–(12) at $\bar{\eta} = 0$. At first glance, application of Lyapunov's indirect method would appear to be quite difficult due to the complexity involved in differentiating the nonlinear functions α and β . However, the processes of “deriving the zero dynamics” and “performing linear approximation” are commutative [3], and hence a much simpler method to evaluate the stability of the equilibrium $\bar{\eta} = 0$ is to compute the zero locations of the transfer function

$$H(z) = C(zI - \Phi)^{-1}\Gamma \quad (13)$$

where

$$\Phi := \left. \frac{\partial F}{\partial x} \right|_{(\bar{x}, \bar{u})} \quad \Gamma := \left. \frac{\partial F}{\partial u} \right|_{(\bar{x}, \bar{u})} \quad C := \left. \frac{\partial h}{\partial x} \right|_{\bar{x}}$$

denote the linear approximation of the original system (1)–(2) at the equilibrium point corresponding to $\bar{y} = 0$, i.e. to $\bar{\eta} = 0$. Presumably, the triple (Φ, Γ, C) is easily obtained and readily available.

Assuming that the equilibrium of interest is hyperbolic, and that there are no pole-zero cancellations in the transfer function, the stability assessment suggested above leads to three possible outcomes. If all the zeros of $H(z)$ are inside the unit circle, then $\bar{\eta} = 0$ is an exponentially stable equilibrium of the zero dynamics and the original system (1)–(2) is said to be *minimum-phase*. If all the zeros of $H(z)$ are outside the unit circle, then $\bar{\eta} = 0$ is an exponentially unstable equilibrium of the zero dynamics and the original system (1)–(2) is said to be *maximum-phase*. If $H(z)$ has zeros both inside and outside the unit circle, then the original system (1)–(2) is said to be (generally) *nonminimum-phase*.

3.5 Numerical Algorithms

Based on the preceding discussion, it is now possible to develop numerical algorithms for solving the stable inversion problem. Throughout this section, assume that the desired output trajectory y_k^d is specified on the interval $k \in [k_i, k_f]$ and, for simplicity, that it begins (at k_i) and ends (at k_f) on a single equilibrium value. This restriction simplifies analysis by confining system trajectories to a neighborhood of a single equilibrium point; however, the following section will demonstrate by simulation that this restriction is not actually necessary.

The main ideas behind the numerical algorithms may be summarized as follows. If the system (1)–(2) is minimum-phase, then its inverse dynamics (9)–(10) will yield a bounded solution $\{u_k, \eta_k\}$ when solved forward in time, for any sufficiently small initial condition η_{k_i} and any sufficiently small desired output trajectory y_k^d . If the system (1)–(2) is maximum-phase, then its inverse dynamics (9)–(10) will yield a bounded solution $\{u_k, \eta_k\}$ when solved backward in time, for any sufficiently small final condition η_{k_f} and any sufficiently small desired output trajectory y_k^d . More generally, if the system (1)–(2) is hyperbolic but nonminimum-phase (i.e. its linear approximation has zeros both inside and outside the unit circle), then its inverse dynamics (9)–(10) will yield a bounded solution $\{u_k, \eta_k\}$ only when solved as a two-point boundary value problem; this general case is not addressed in this paper.

Consider first the minimum-phase case. Viewing the inverse dynamics as a perturbation of the zero dynamics, exponential stability of the zero dynamics equilibrium $\bar{\eta} = 0$ implies that the inverse dynamics is locally input-to-state stable [6]. Consequently, inverse dynamics solutions computed forward in time will be bounded for sufficiently small initial condition and desired output trajectory. Newton iteration may be used to handle the nonlinearity of α with respect to u_k as follows.

Given desired output trajectory y_k^d and initial condition $\eta_{k_i} = 0$, the following steps are performed for each incrementing value of $k \in [k_i, K_f]$ where $K_f > k_f$ is selected large enough to ensure that the bounded solution reaches equilibrium: (i) beginning with an initial estimate of u_k , the iteration

$$u_k^{(j+1)} = u_k^{(j)} - \frac{\alpha(\zeta_k^d, \eta_k, u_k^{(j)}) - y_{k+r}^d}{\frac{\partial \alpha}{\partial u}(\zeta_k^d, \eta_k, u_k^{(j)})}$$

is used until convergence occurs, limiting the step size if necessary; and (ii) the value of η_k is updated according to

$$\eta_{k+1} = \beta(\zeta_k^d, \eta_k, u_k)$$

This computational procedure will be referred to as the *minimum-phase stable inversion algorithm*. It provides bounded desired input-state trajectory $\{u_k, x_k\} = \{u_k, \varphi^{-1}(\zeta_k^d, \eta_k)\}$ over the interval $k \in [k_i, K_f]$. Note that division by zero in the Newton iteration should not occur by virtue of the relative degree assumption.

Since the inverse dynamics is solved as an initial-value problem, it is possible to impose equilibrium on the interval $k \leq k_i$. On the other hand, the output of the minimum-phase stable inversion algorithm will not typically be at equilibrium over the entire interval $k \geq k_f$. Instead, inside the interval $k \in [k_f, K_f]$ some decaying transient response (satisfying the zero dynamics) will be present. This effect may be referred to as *post-actuation*, implying that some transient feedforward excitation will generally be required to achieve exact tracking even after the output motion has stopped.

Now consider the maximum-phase case, the main topic of this paper. The previous section established the fact that, for this case, the linear approximation of the zero dynamics at the equilibrium $\bar{\eta} = 0$ has all eigenvalues strictly outside the unit circle. It follows that the linear approximation of the time-reversed zero dynamics at the equilibrium $\bar{\eta} = 0$ has all eigenvalues strictly inside the unit circle. Since the time-reversed zero dynamics possesses an exponentially stable equilibrium, the time-reversed inverse dynamics will be locally input-to-state stable. Thus, in order to obtain a bounded solution $\{u_k, \eta_k\}$, it is necessary to solve the inverse dynamics backward in time for maximum-phase systems.

Because of time-reversal the nonlinearities of both α and β , with respect to both η_k and u_k , add complexity to the numerical algorithm. The inverse dynamics may be viewed as a set of coupled nonlinear algebraic equations. The number of equations and the number of unknowns are both equal to $n - r + 1$. Given desired output trajectory y_k^d and final condition $\eta_{k_f} = 0$, Newton iteration will be applied for each decrementing value of $k \in [K_i, k_f]$ where $K_i < k_i$ is selected small enough to ensure that the bounded solution reaches equilibrium. The

Newton iteration, initialized with estimates of η_k where and u_k , is given by

$$\begin{bmatrix} \eta_k^{(j+1)} \\ u_k^{(j+1)} \end{bmatrix} = \begin{bmatrix} \eta_k^{(j)} \\ u_k^{(j)} \end{bmatrix} - \left(J_k^{(j)} \right)^{-1} \cdot \left(f_k^{(j)} - \begin{bmatrix} y_{k+r}^d \\ \eta_{k+1} \end{bmatrix} \right)$$

where

$$f_k^{(j)} := \begin{bmatrix} \alpha \left(\zeta_k^d, \eta_k^{(j)}, u_k^{(j)} \right) \\ \beta \left(\zeta_k^d, \eta_k^{(j)}, u_k^{(j)} \right) \end{bmatrix}$$

$$J_k^{(j)} := \frac{\partial f_k^{(j)}}{\partial (\eta, u)}$$

and is used until convergence occurs, limiting the step size if necessary. This computational procedure will be referred to as the *maximum-phase stable inversion algorithm*. It provides bounded desired input-state trajectory $\{u_k, x_k\} = \{u_k, \varphi^{-1}(\zeta_k^d, \eta_k)\}$ over the interval $k \in [K_i, k_f]$. The nonsingularity of the Jacobian matrix follows from the assumptions of relative degree and maximum-phase.

Since the inverse dynamics is solved as a final-value problem, it is possible to impose equilibrium on the interval $k \geq k_f$. On the other hand, the output of the maximum-phase stable inversion algorithm will not typically be at equilibrium over the entire interval $k \leq k_i$. Instead, inside the interval $k \in [K_i, k_i]$ some decaying transient response (satisfying the zero dynamics) will be present. This effect may be referred to as *pre-actuation*, implying that some transient feedforward excitation will generally be required to achieve exact tracking even before the output motion has begun.

4 Simulation Examples

Switched-mode power converters operate on the basis of pulse-width modulation [5]. For example, a single-switch power converter that operates exclusively in continuous conduction mode will alternate between two topologies (A_1, B_1) and (A_2, B_2) with switching period T and hence may be modeled by

$$x_{k+1} = F(d_k)x_k + G(d_k)u_k \quad (14)$$

$$y_k = Cx_k \quad (15)$$

where $x_k := x(kT)$ and $y_k := y(kT)$ denote sample values, and where the source input has been assumed to be piecewise-constant, i.e. $u(t) =: u_k$ for all $t \in [kT, kT + T)$. The control input d_k is the switch duty ratio and enters the open-loop dynamics through the functions

$$F(d) := \Phi_2((1-d)T)\Phi_1(dT)$$

$$G(d) := \Phi_2((1-d)T)\Gamma_1(dT) + \Gamma_2((1-d)T)$$

$$\Phi_i(t) := e^{A_i t}$$

$$\Gamma_i(t) := \int_0^t e^{A_i \tau} B_i d\tau$$

The discrete-time model (14)–(15) is clearly nonlinear, especially for the larger values of switching period T that may be required when using higher-power semiconductor switches.

To be more specific, consider the lossless buck-boost converter. State variables $x_1(t)$ and $x_2(t)$ are selected to be the inductor current and the capacitor voltage, respectively, and $u(t) = V_g$ represents the constant voltage applied by the dc source. The output $y(t)$ is the voltage delivered to the resistive load, and hence $y(t) = x_2(t)$. For the numerical example, the parameter values are $R = 10 \Omega$, $L = 2 \text{ mH}$, $C = 200 \mu\text{F}$, $V_g = 100 \text{ V}$ and $T = 200 \mu\text{s}$. With these parameter values, the nonlinear discrete-time model (14)–(15) has relative degree one and is maximum-phase; the zero of the linear approximate model corresponding to the equilibrium defined by $\bar{d} = 0.5$ is located at $z = 1.8562$.

The stable inversion theory may be applied to the buck-boost converter by following the general approach outlined in the previous section. However, since for this example the output is equal to one of the state variables and the relative degree is unity, no coordinate transformation is really necessary to form the inverse dynamics. In fact, the inverse dynamics may be written in the implicit form

$$\begin{bmatrix} x_{1,k+1}^d \\ y_{k+1}^d \end{bmatrix} = F(d_k^d) \begin{bmatrix} x_{1,k}^d \\ y_k^d \end{bmatrix} + G(d_k^d) V_g \quad (16)$$

thus providing two constraint equations for the two unknowns $x_{1,k}^d$ and d_k^d , where $x_{1,k+1}^d$ is known at time k due to the time-reversed solution method. Note that the first constraint in (16) is a dynamic equation, corresponding to (10), whereas the second constraint in (16) is a static equation, corresponding to (9). The maximum-phase stable inversion algorithm may be applied directly to (16) in order to compute a bounded input-state trajectory consistent with the given output trajectory y_k^d .

The first simulation considers dc-to-dc power conversion. The desired trajectory is specified to be a transition from the output corresponding to $\bar{d} = 0.3$ to the output corresponding to $\bar{d} = 0.7$, with transition time of $30T = 6 \text{ ms}$. Since the converter is open-loop stable, the inversion scheme is easily assessed by computing the inversion accuracy using only the feedforward input alone. The result is shown in Fig. 1. Note that the desired input d_k^d exhibits a distinct pre-actuation effect lasting 1.8 ms or 9 switching periods. Both the desired state trajectory x_k^d and the actual state trajectory using feedforward only are displayed on the same axes;

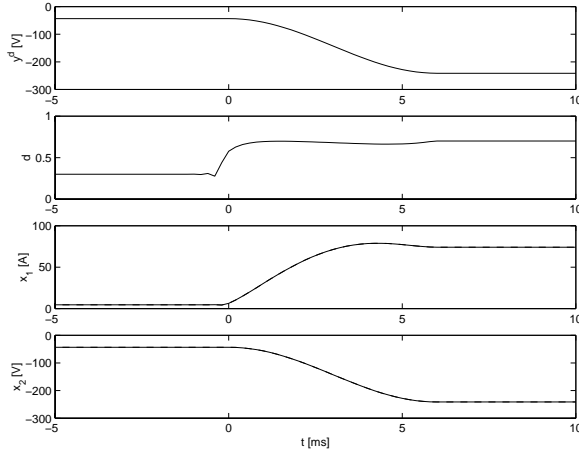


Figure 1: DC-DC conversion with stable inversion.

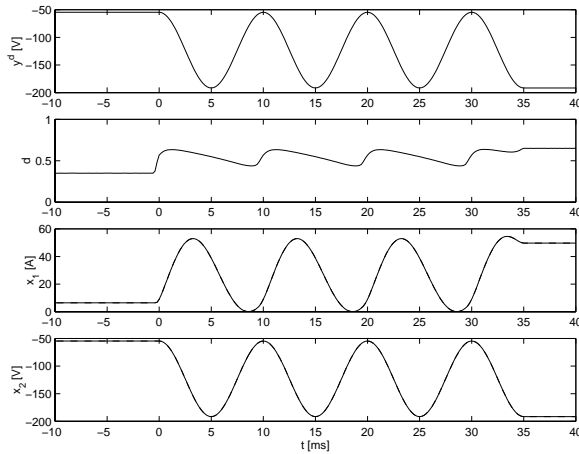


Figure 2: DC-AC conversion with stable inversion.

on the given scale, the plots are indistinguishable. The inductor current trajectory exhibits both the pre-actuation effect and some overshoot in the approach to its final value. Instantaneous output error is on the order of 10^{-12} V, due only to small numerical errors in the sampled-data model itself and the Newton iteration method.

To further demonstrate the value of the maximum-phase stable inversion algorithm, it has also been used to achieve dc-to-ac power conversion. The results are shown in Fig. 2. In this simulation, the peak values of the ac output voltage correspond to the equilibria defined by $\bar{d} = 0.35$ and $\bar{d} = 0.65$, and the period of the oscillation is equal to $50T = 10$ ms. The instantaneous output error achieved is on the order of 10^{-11} V. The required input trajectory is extremely non-sinusoidal and would likely be difficult to predict without using the maximum-phase stable inversion algorithm. This particular trajectory requires inductor currents that nearly approach zero and hence nearly

lead to the discontinuous conduction mode of operation.

5 Conclusions

This paper has presented numerical algorithms for the stable inversion of either minimum-phase or maximum-phase discrete-time nonlinear systems. The discrete-time theory of this paper differs from the continuous-time theory of [1, 2] in several significant ways, including (i) the need to account for nonlinearity in the plant state equation with respect to the control input due to the effects of sampling and (ii) the need for iterative schemes such as Newton's method for solving nonlinear equations (1 equation for the minimum-phase case and $n - r + 1$ simultaneous equations for the maximum-phase case). Although the general idea of solving the stable part of the inverse dynamics in forward time and solving the unstable part of the inverse dynamics in reverse time is common between the continuous-time and discrete-time stable inversion formulations, the actual mechanisms for time-reversal in the two cases are quite different.

In addition to developing the new theory outlined above, this paper also includes a practical application of stable inversion to switched-mode power converters. Since such converters are operated by pulse-width modulation, it is natural to design their control systems using discrete-time methods. Several classical converter topologies give rise to maximum-phase nonlinear discrete-time models, including the buck-boost topology considered in the simulation examples.

References

- [1] D. Chen and B. Paden, "Stable inversion of nonlinear non-minimum phase systems," *International Journal of Control*, 64, 81–97, 1996.
- [2] S. Devasia, D. Chen and B. Paden, "Nonlinear inversion-based output tracking," *IEEE Transactions on Automatic Control*, 41, 930–942, 1996.
- [3] A. Isidori, *Nonlinear Control Systems*, Second Edition. Springer-Verlag, New York, NY, 1989.
- [4] A. Isidori and C. I. Byrnes, "Output regulation of nonlinear systems," *IEEE Transactions on Automatic Control*, 35, 131–140, 1990.
- [5] J. G. Kassakian, M. F. Schlecht and G. C. Verghese, *Principles of Power Electronics*. Addison-Wesley, Reading, MA, 1991.
- [6] H. K. Khalil, *Nonlinear Systems*. Macmillan, New York, NY, 1992.